2026 S.T. Yau High School Science Award (Asia)
Research Report

The Team

Registration Number: **Chem-173**

Name of team member: LIAO,BO-JUN

School: The Affiliated Senior High School of Taiwan Normal University

Name of supervising teacher: YEH,SHIH-CHAO

Job Title: Chemistry teacher

School: The Affiliated Senior High School of Taiwan Normal University

Title of Research Report

Skeletal Geometry × Steric-Electronic Effects: Unlocking the Performance Code of Rh(I)-Catalyzed Asymmetric Cyclization

Date

17 August 2026

2026 S.-T. Yau High School Science Award
仅用于2026丘成桐中学科学奖论文公示

Skeletal Geometry × Steric-Electronic Effects: Unlocking the Performance Code of Rh(I)-Catalyzed Asymmetric Cyclization

LIAO,BO-JUN

Abstract

This study unlocks the "performance code" of Rh(I)-catalyzed asymmetric cyclization by systematically decoupling the structural and environmental factors that govern catalytic efficiency. Through precisely controlled experiments, we established a definitive hierarchy of four key effects: Skeletal Geometry > Steric Effect > Electronic Effect > Temperature Effect.

We identified that **skeletal geometry** is the absolute determinant of regioselectivity. The rigid bicyclo[2.2.1]heptadiene framework proved to be the optimal backbone, achieving an ultra-high regioselectivity of >20:1, whereas monocyclic or bicyclo[2.2.2] frameworks led to a drastic decline or complete reversal in selectivity. Furthermore, **steric effects** primarily dictate enantioselectivity (ee), with symmetric diaryl substitutions significantly enhancing chiral recognition. **Electronic effects** serve as a fine-tuning mechanism, where electron-donating groups marginally improve both yield and ee, while **temperature** acts solely as an external accelerator without altering intrinsic selectivity.

Significantly, we translated these empirical findings into a robust, semi-quantitative prediction model. By parameterizing the four effects into quantitative indices (F1–F4) and utilizing advanced hurdle and two-part regression techniques to resolve data zero-inflation and ceiling effects, our model accurately predicts core reaction metrics, including regioselectivity, ee, yield, and reaction time. This research not only elucidates the deep mechanistic relationship between ligand architecture and catalytic activity but also provides a pioneering, predictive framework for the rational design of next-generation high-performance chiral catalysts.

Keywords: Rhodium catalysis, Asymmetric catalysis, Chiral ligand

2026 S.-T. Yau High School Science Award
仅用于2026丘成桐中学科学奖公示

Acknowledgement

Sincere thanks to Professor Hsueh Liang Wu and the Organic Laboratory for their expert advice and provision of experimental resources during this study.

AI usage: None

Note: This work is also entered in the 66th Science Fair in Taiwan.

2026 S.-T. Yau High School Science Award
仅用于2026丘成桐中学科学奖论文公示

Commitments on Academic Honesty and Integrity
We hereby declare that we

1. are fully committed to the principle of honesty, integrity and fair play throughout the competition.
2. perform the research work ourselves and thus truly understand the content of the work.
3. observe the common standard of academic integrity adopted by most journals and degree theses.
4. have declared all the assistance and contribution we have received from any personnel, agency, institution, etc. for the research work.
5. have truthfully disclosed all AI tool usage in the research report and obtained prior approval from supervising teachers. All supporting documentation has been submitted as required. We hereby affirm that no improper use of AI has occurred at any stage of the research process.
6. undertake to avoid getting in touch with assessment panel members in a way that may lead to direct or indirect conflict of interest.
7. undertake to avoid any interaction with assessment panel members that would undermine the neutrality of the panel member and fairness of the assessment process.
8. observe the safety regulations of the venue(s) where we conduct the experiment(s), if applicable.
9. observe all rules and regulations of the competition.
10. agree that the decision of YHSA(Asia) is final in all matters related to the competition.

We understand and agree that failure to honor the above commitments may lead to disqualification from the competition and/or removal of award, if applicable; that any unethical deeds, if found, will be disclosed to the school principal of the team member(s) and relevant parties if deemed necessary; and that the decision of YHSA(Asia) is final and no appeal will be accepted.

(Signatures of full team below)
Name of team member:

Name of supervising teacher:

Noted and endorsed by
(signature)

Name of school principal:

2026 S.T. Yau High School Science Award
仅用于2026丘成桐中学科学奖论文公示

Table of Contents

Abstract 1

Acknowledgement 2

Commitments on Academic Honesty and Integrity 3

1. Research Motivation 5

2. Research Objectives and Questions 6

3. Chemicals, Materials, and Equipment 7

4. Experimental Design and Methodology 11

5. Results and Discussion 15

6. Prediction Model (Two-part / Hurdle Regression) 19

7. Conclusion 24

References 24

Appendix 24

2026 S.-T. Yau High School Science Award
仅用于2026丘成桐中学科学奖论文公示

1. Research Motivation

In contemporary drug discovery, the precise and highly efficient synthesis of chiral target molecules is a core technology. Since different enantiomers often exhibit entirely distinct biological activities, strict stereochemical control is crucial. Recently, asymmetric catalysis has become a highly attractive synthetic strategy due to its operational convenience, good yields, and excellent selectivity, sparking our intense interest in exploring catalytic mechanisms.

Extensive literature indicates that transition metal complexes play a pivotal role in driving asymmetric catalysis. Among them, rhodium (Rh)-based catalytic systems demonstrate exceptional stereocontrol and reactivity in various asymmetric reactions. For instance, the Hayashi group in 2005 pioneered a catalytic system comprising Rh(I) and chiral dienes, successfully achieving highly enantioselective conjugate addition of arylboronic acids to α,β-unsaturated carbonyl compounds (Conditions: $[RhCl(C_2H_4)_2]_2$ 5 mol%, chiral diene 5.5 mol%, KOH as base, solvent 1,4-dioxane/H_2O = 10:1, temperature 35 °C). Since 2011, a new generation of C_2-symmetric chiral bicyclic diene ligands has been developed, which retains structural rigidity while significantly enhancing enantioselectivity by fine-tuning remote sterics and electronic effects. These achievements established vital design rules: ligand spatial geometry (e.g., bite angle and rigidity), electronic environment, and steric hindrance are primary determinants of stereoselectivity.

Building upon this foundation, this research focuses on the molecular design of catalysts. We utilize arylboronate esters and asymmetric alkynes as starting materials for Rh-catalyzed reactions. We systematically synthesized diverse ligand molecules and coordinated them with rhodium centers to compare their structural impact on yield and ee. We aim to decode the deeper relationship between catalytic activity and molecular structure, thereby establishing design-oriented catalytic principles.

2026 S.T.You High School Science Award
仅用于2026年度中学科学奖公示

2. Research Objectives and Questions

Objectives:

Using three typical geometric structures of diene ligands (monocyclic diene, bicyclo[2.2.1]heptadiene, and bicyclo[2.2.2]octadiene) as research subjects, we compare experimental data to clarify the regulatory patterns and strengths of skeletal geometry on four core reaction metrics, providing experimental and theoretical support for the skeleton design of high-performance chiral ligands.

Research Questions:

- How do ligand types and configurations influence the regioselectivity and enantioselectivity of the products?
- How do the interactions between the ligand and the metal center during the reaction affect the mechanism and selectivity?
- Can a mathematical model be used to predict regioselectivity and enantiomeric excess (ee)?

2026 S.-T. Yau High School Science Award
仅用于2026丘成桐中学科学奖论文公示

3. Chemicals, Materials, and Equipment

3.1 Research Equipment

Equipment	Model	Equipment	Model
Rotary Evaporator	MZ 2C NT	TLC Plates	Xtra SIL G UV254
Vacuum System	Custom	Column Chromatography Setup	Self-assembled
Vacuum Distillation Setup	Self-assembled	NMR Spectrometer	N/A
Chiller	LRB-80	HPLC	LC-2050C-3D
Magnetic Stirrer/Heater	MR Hei-Tec	UV Lamp	UVGL-25
Heat Gun	TS-2200	Dry Solvent System	AWP-SOL-A-5
Analytical Balance	ATY224R	Glove Box	SG1200
Air Pressurizer	EP-9000		

2026 S.-T. Yau High School Science Award
仅用于2026丘成桐中学科学奖论文公示



Figure 1. Column chromatography setup



Figure 2. Rotary evaporator

2026 S. Tianjin English School Science Award
仅用于2026天津英华科学奖公示

3.2 Chemicals

Chemical	Brand	Chemical	Brand
Bis(pinacolato)diboron	AK Scientific	NH_4Cl (aq)	Self-prepared
Potassium Acetate (KOAc)	Showa	Nitrogen (N_2)	Yousheng
Triphenylphosphine (PPh_3)	TCI	$[RhCl(C_2H_4)_2]_2$	Morrchem
Palladium Acetate $Pd(OAc)_2$	Morrchem	Aryl Boronate	Self-synthesized
1,4-Dioxane	Thermo	Asymmetric Alkyne	Self-synthesized
Ethyl Acetate (EA)	DUKSAN	Sodium Carbonate (Na_2CO_3)	Liangong
n-Hexane	Honeywell	Silica Gel (SiO_2)	KM3
Toluene	Fisher chemical	$KMnO_4$ Solution	Self-prepared
Ether	Duksen	Argon (Ar)	Yousheng
Dichloromethane (DCM)	Thermo	2-Aminopyridine	TCI
tert-Butyl Acetate (t-BuOAc)	TCI	Pyridine	Thermo

2026 S.T. Yau High School Science Award
仅用于2026丘成桐中学科学奖论文公示

Sat. NaCl (aq)	Self-prepared	Trifluoromethanesulfonic Anhydride (Tf_2O)	Nova
Triflic Acid (TfOH)	SIGMA	NaOH	Showa
Ethanol (EtOH)	ECHO	Methyl 2-(triphenylphosphoranylidene)acetate	BLD
Triethylamine (Et_3N)	ECHO	Phenylpropiolic acid	TCI
H_2O		Tetrahydrofuran (THF)	Macron
2'-Bromoacetophenone	AK Scientific	KHMDS	Thermo

2026 S.-T. Yau High School Science Award
仅用于2026丘成桐中学科学奖论文公示

4. Experimental Design and Methodology

Study of Skeletal Geometry Effects:
To explore the regulatory patterns of ligand skeletal geometry on regioselectivity, enantioselectivity (ee), isolated yield, and reaction rate. We performed parallel catalytic experiments changing only the ligand skeleton (monocyclic, bicyclo[2.2.1], bicyclo[2.2.2]) while keeping other conditions constant ($[RhCl(C_2H_4)_2]_2$ catalyst 3.0 mol%, ligand 3.6 mol%, Na_2CO_3 2 equiv., Dioxane:H_2O=10:1, substrate 0.2 mmol, base temp 30 °C).

4.1 Synthesis of Starting Materials

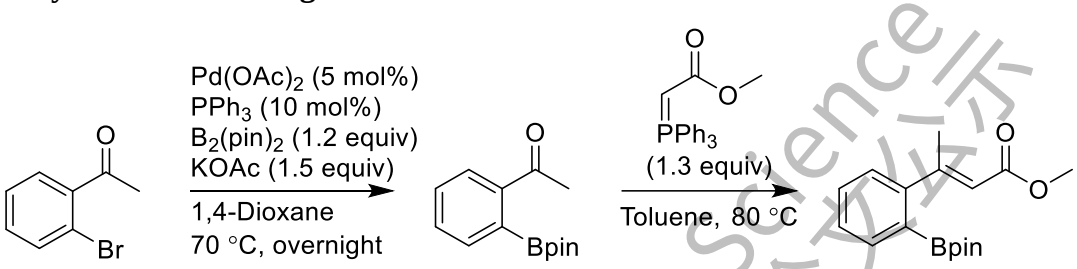


Figure 3. Synthesis steps of aryl boronate

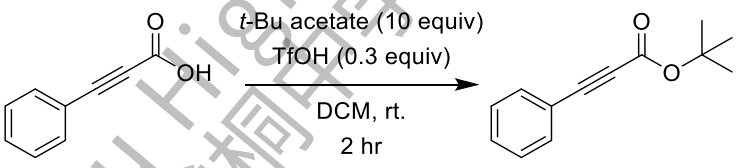


Figure 4. Synthesis steps of isobutyl phenylpropiolate

4.2 Ligand Synthesis

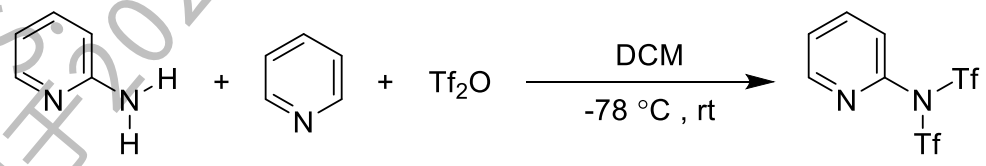


Figure 5. Synthesis of Comins' reagent

2026 S. T. Yau High School Science Award
仅用于2026丘成桐中学科学奖论文公示

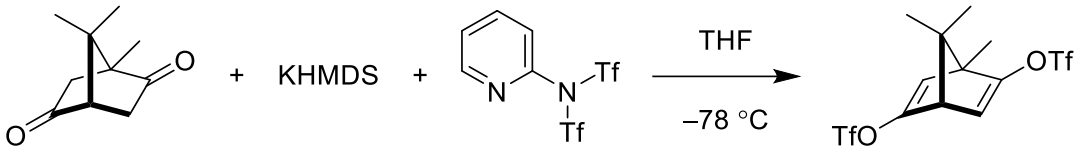


Figure 6. Synthesis of bistriflate

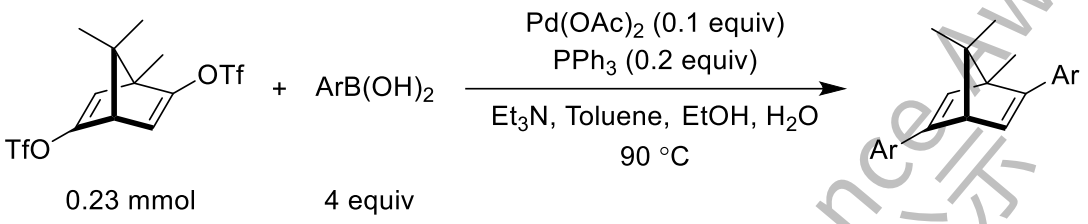


Figure 7. Ligand synthesis (Ar= Ph, 4-tBu-Ph, 4-NO2-Ph, 4-OMe-Ph, 2-Naphthyl)

4.3 Rhodium Catalysis and Mechanism

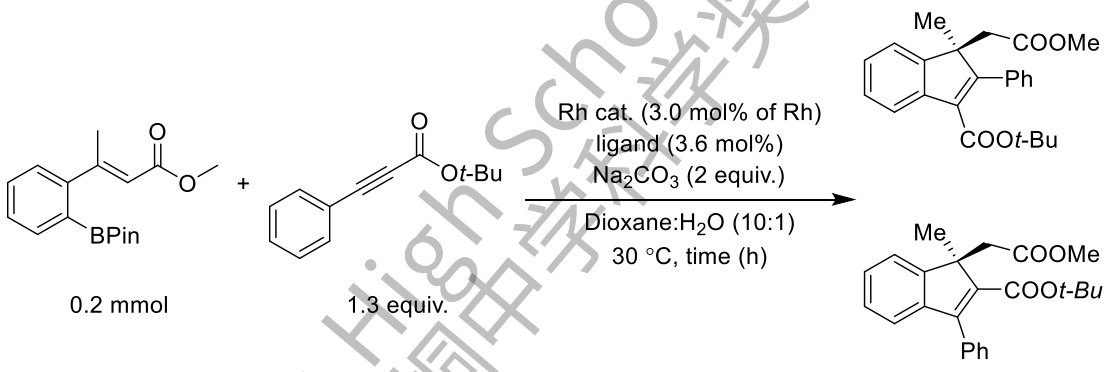


Figure 8. Rhodium catalysis

Reaction Mechanism:

Based on literature mechanisms and the conditions of this study, the Rh-catalyzed asymmetric conjugate addition can be described by the following steps (see Figure "Reaction Mechanism"):

1. **Catalyst Activation and Formation of Hydroxorhodium Species:** In an aqueous basic environment, the precursor catalyst [Rh] reacts with water and a base to transform into the catalytically active [Rh]–OH intermediate. This step initiates the catalytic cycle, imparting reactivity to the metal center for subsequent transmetalation.

2026 Siyau High School Science Award
仅用于2026斯育成绩申请奖论文公示

2. **Transmetalation:** Assisted by the base, arylboronic acid (or arylboronate ester) undergoes transmetalation with [Rh]–OH, transferring the aryl group (Ar) from the boron atom to the rhodium metal center to generate the key active Ar–[Rh] intermediate.
3. **Coordination and Insertion / 1,4-Conjugate Addition:** The carbon–carbon double bond of the α,β-unsaturated carbonyl substrate (such as enones or enoates) first coordinates to the rhodium metal center. Subsequently, migratory insertion occurs (macroscopically equivalent to a 1,4-conjugate addition), transferring the aryl group (Ar) to the β-carbon of the substrate to form a rhodium enolate intermediate.
4. **[Intramolecular Cyclization and Enantioselectivity Control]:** If the substrate possesses appropriate stereoelectronic configurations, the newly formed enolate intermediate can undergo further intramolecular coordination or addition to yield a temporarily stable five-membered rhodacycle (Intermediate III in the figure). During this process, the chiral pocket constructed by the ligand governs the stereoselectivity of the reaction through precise control of steric hindrance and coordination geometry.
5. **Protonolysis and Catalyst Regeneration:** Finally, this metallacycle intermediate undergoes protonolysis by a water molecule to release the target chiral 1,4-addition product while simultaneously regenerating the active [Rh]–OH species to complete the catalytic cycle.

2026 S.-T. Yau High School Science Award
仅用于2026丘成桐中学科学奖论文公示

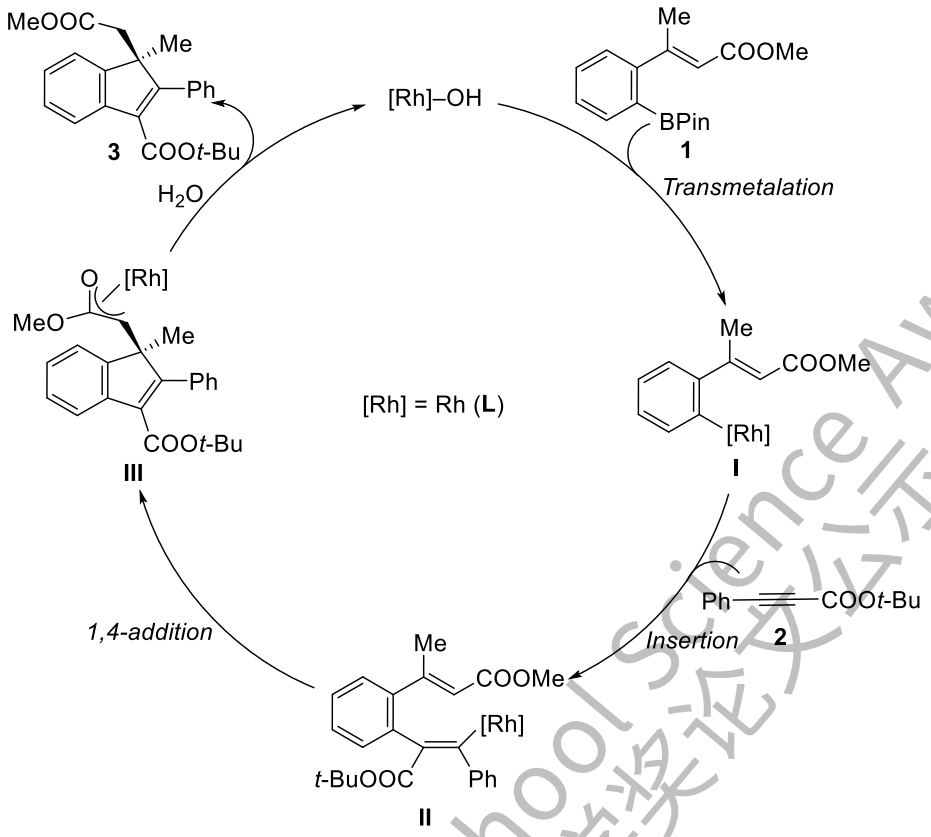
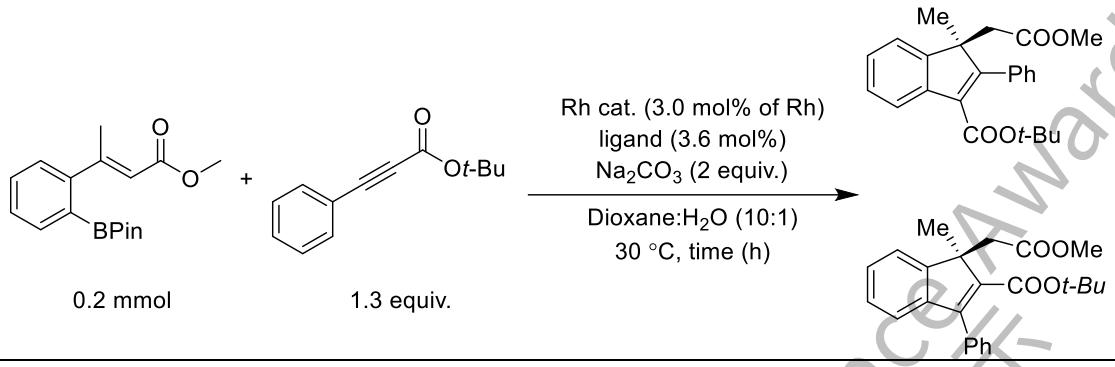


Figure 9. Reaction mechanism

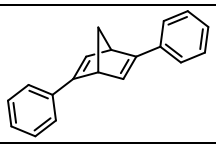
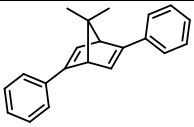
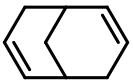
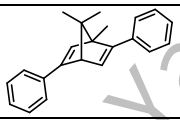
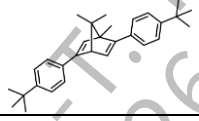
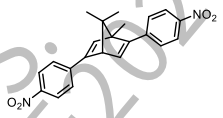
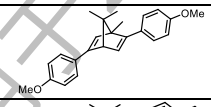
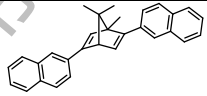
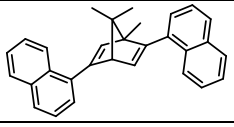
2026 S.-T. Yau High School Science Award
仅用于2026丘成桐中学科学奖论文公示

5. Results and Discussion

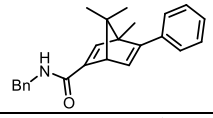
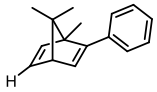
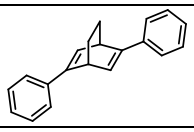
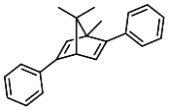
5.1 Catalytic Performance Data



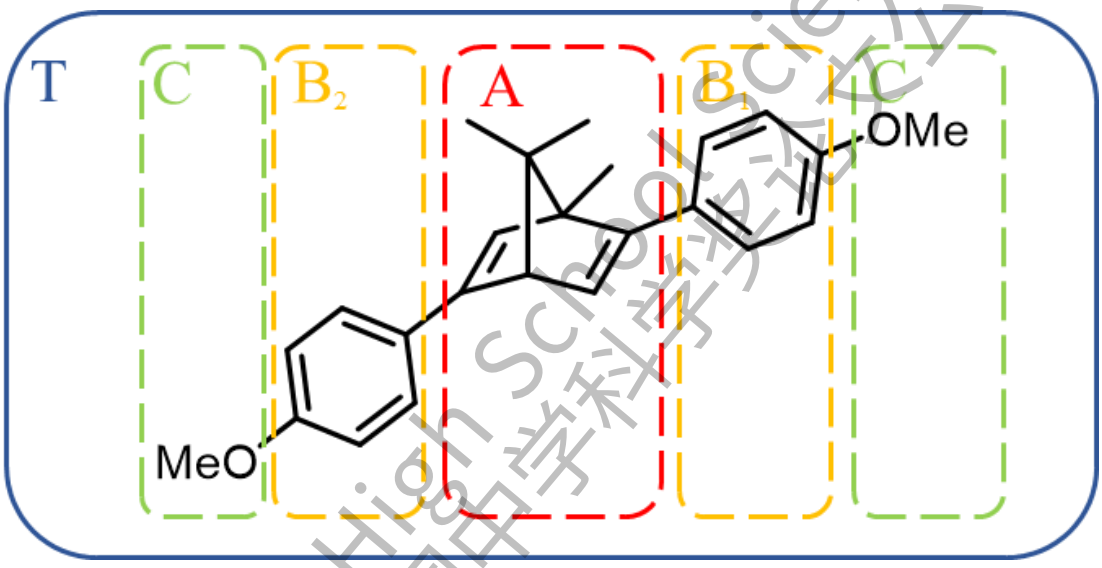
0.2 mmol 1.3 equiv.

Entry	Ligand Type (Skeleton)	Temp. (°C)	Time (h)	Ratio[a] of 3:4	Isolated Yield(%) of **3**+**4**	ee(3, %)	ee(4, %)
A		30	24	5.7:1	44	—	—
B		30	8	1:4	95	—	—
C		60	6	7:1	—	—	—
D		60	6	1:1.1	—	—	—
E		60	6	1.6:1	—	—	—
1		30	6	>20:1	93	95	—
2		30	24	>20:1	64	89.5	—
3		30	8	>20:1	96	94	—
4		30	8	>20:1	>99	97.5	—
5		30	6	>20:1	89	90	—
6		30	8	—	—	—	—

2026 S.-T. Yau High School Science Award
仅用于2026丘成桐中学科学奖论文公示

7		30	6	4.4:1	94	92	16
8		30	6	2.4:1	97	74	12
9		30	6	3:1	85	15.5	3.5
T1		60	4	>20:1	91	96	—
T2		30	6	>20:1	93	95	—

Note 1: The top is Product 3, and the bottom is Product 4.
Note 2: Entry 6 is known laboratory data.



A: Skeletal Geometry B: Steric Strain C: Electronic effect T: Temperature effect

5.2 Skeletal Geometry Effect (Structural Determinant)

This is the primary regulatory factor. The rigidity and geometry of the ligand skeleton dictate the spatial orientation of the Rh center. The bicyclo[2.2.1]heptadiene structure acts as the optimal rigid bridged skeleton. When appropriately substituted, it restricts substrate approach exclusively to the 3-position, yielding an ultra-high regioselectivity (>20:1) and establishing the foundational chiral pocket required for high ee. The more flexible bicyclo[2.2.2] skeleton causes a severe drop in both regioselectivity (3:1) and ee (15.5%), while the monocyclic skeleton reverses regioselectivity altogether (1:4).

2026 S. T. Yau High School Science Award
仅用于2026丘成桐中学科学奖公示

Ligand Skeleton Geometry	Rep. Entry	Regioselectivity (3:4)	ee(3) (%)	Isolated Yield (%)	Time (h)	Performance Eval.
Unsubstituted Bicyclo[2.2.1]	A	5.7:1	-	44	24	Extremely poor
Substituted Bicyclo[2.2.1]	1/3/4/T2	>20:1	≥94	≥93	6~8	Excellent (Optimal)
Bicyclo[2.2.2]	9	3:1	15.5	85	6	Poor selectivity
Monocyclic (Cyclooctadiene)	B	1:4	-	95	8	Reversed selectivity

Figure 10. Experimental data support table (Core skeleton comparison)

5.3 Steric Effect (Core Chiral Regulator)

Operating upon the optimal [2.2.1] skeleton, the steric bulk and symmetry of the aryl substituents govern enantioselectivity. Symmetric diaryl substitution creates a well-defined, symmetric chiral environment. Mono-substitution or asymmetric substitution compromises the chiral pocket, reducing ee and regioselectivity. However, excessive steric bulk significantly hampers reaction rates and lowers yield due to restricted substrate access.

Steric Type	Regioselectivity (3:4)	ee(3) (%)	Yield (%)	Time (h)
Mono-phenyl	2.4	74	97	6
Asymmetric	4.4	92	94	6
Symmetric Diphenyl	20	95	93	6

2026 S.T.Yau High School Science Award
仅用于2026丘成桐中学科学奖论文公示

Symmetric Di-p-tBu-phenyl	20	89.5	64	24
Symmetric Di-2-naphthyl	20	90	89	6

Figure 11. Comprehensive data of Steric Effect

5.4 Electronic Effect (Fine-Tuning Mechanism)

This effect provides fine-tuning without altering the dominant selectivity preferences set by geometry and sterics. Electron-donating groups (e.g., -OCH_3) increase electron density on the transition state, modestly enhancing both yield (>99%) and ee (97.5%). The electronic nature noticeably affects the reaction rate by modulating substrate activation efficiency.

Electronic Property	**Regioselectivity (3:4)**	**ee(3) (%)**	**Yield (%)**	**Time (h)**
Neutral (Phenyl)	20	95	93	6
Electron-withdrawing	20	94	96	8
Electron-donating	20	97	99	8

Figure 12. Comprehensive data of Electronic Effect

5.5 Temperature Effect (External Accelerator)

Raising the temperature from 30 °C to 60 °C drastically reduced reaction time from 6h to 4h without compromising the core regioselectivity (>20:1). Variations in ee and yield were negligible, validating temperature as a reliable external tool strictly for rate optimization.

2026 S.-T. Yau High School Science Award
仅用于2026丘成桐中学科学奖论文公示

6. Prediction Model (Two-part / Hurdle Regression)

Based on the regulatory rules established by the four major effects, we constructed a semi-quantitative prediction model utilizing an "Effect Factor Quantification + Empirical Fitting" approach. This model aims to translate adjustable reaction parameters into predictive outputs for the core metrics.

6.1 Variable Definition and Quantitative Coding (F1–F4)

To build an interpretable statistical model for the asymmetric induction capability of the ligand structures, the ligand features were decomposed into four indices based on prior chemical mechanisms, employing ordinal scoring:

- **F1 (Skeletal Geometry / Chiral Origin):** Scored based on the main skeleton and whether it provides an effective chiral pocket. (e.g., Substituted Bicyclo[2.2.1] = 5; Unsubstituted Bicyclo[2.2.1] = 2; Bicyclo[2.2.2] = 1; Monocyclic = 0).
- **F2 (Steric Topology / Pocket Completeness):** Scored based on the 2,5-substitution pattern, symmetry, and steric hindrance. (e.g., Symmetric standard aryl = 5; Asymmetric = 4; Bulky symmetric = 3; Mono-aryl = 2; No aryl/No effective environment = 0).
- **F3 (Electronic/Polarity Effect):** Scored based on the electron-donating/withdrawing properties. (e.g., Electron-donating = 4; Electron-withdrawing = 3; Neutral/Phenyl = 2).
- **F4 (Temperature):** Represented as discrete levels (e.g., 60 °C = 4; 30 °C = 2).

2026 S.-T. Yau High School Science Award
仅用于2026丘成桐中学科学奖论文公示

Output Core Metric	Positive Trend Criteria	Optimal Factor Combination	Failure/Deterioration Trend
Regioselectivity (3:4)	$F_1 \geq 5$ & symmetric substitution → Ultra-high selectivity (>20:1); $F_1 < 5$ → Selectivity drops drastically/reverses	$F_1=5$(Substituted bicyclo[2.2.1])	$F_1 \leq 2$ → Directly judged as 3:4 < 5.7:1 or 1:4
Enantioselectivity ee(3)	$F_1=5$ + $F_2 \geq 4$ → ee≥90%;$F_2<4$ → ee<90%	$F_1=5$ + $F_2=5$ + $F_3=4$(Optimal skeleton + Symmetric aryl + Electron-donating)	$F_1 \neq 5$ → Directly judged as ee≈0 or <20%
Isolated Yield	$F_1=5$ + $F_2 \geq 3$ + $F_3 \geq 2$ → Yield ≥89%;$F_2=3$ → Yield decreases	$F_1=5$ + $F_2=5$ + $F_3=4$	$F_1=2$ (Unsubstituted skeleton) → Yield ≤50%
Reaction Rate (Time)	$F_4=4$ (60°C) → Fastest rate;$F_2=3$ → Rate slows drastically	$F_1=5$ + $F_2=5$ + $F_4=4$	$F_2=3$ (Bulky sterics) → Reaction time ≥20h

These indices (F1–F4) are ordinal classifications; their numerical values represent rank orders rather than equidistant physical quantities. The regression coefficients are used to describe trend directions and relative impact.

6.2 Two-part (Hurdle) Model for Enantiomeric Excess (ee% of 3)

In our dataset, the **ee(3, %)** exhibits a significant **zero-inflation** phenomenon: certain ligand combinations completely fail to form an effective asymmetric control state, resulting in ee(3, %) = 0. However, when successful (ee > 0), the values cluster in the high ee range. A single linear regression would be strongly skewed by the zero values, diminishing its ability to model the successful states. Thus, a two-part (hurdle) model was adopted to separately model "whether an asymmetric induction is successful" and "the magnitude of ee upon success".

2026 S.T. Yau High School Science Award
仅用于2026丘成桐中学科学奖公示

Let $S = 1$ if $ee(3, \%) > 0$ (Success = 1, Failure = 0).

Part 1: Probability of Success (Logistic Regression)

$$p = \Pr(S = 1) = \frac{1}{1 + \exp(-z)}$$

$$z = \beta_0 + \beta_1 F1 + \beta_2 F2 + \beta_3 F3 + \beta_4 F4 z$$

The estimated coefficients based on this study's data are

$$z = -5.5024 + 0.9911 \times F1 + 0.8719 \times F2 - 0.0315 \times F3 + 0.0394 \times F4$$

Part 2: Magnitude of ee under Success (Ridge Linear Regression)

In the subset where $S = 1$, L2 regularized linear regression (Ridge, α=10) was used to estimate the magnitude of the successful ee.

$$ee_{pos} = \gamma_0 + \gamma_1 F1 + \gamma_2 F2 + \gamma_3 F3 + \gamma_4 F4$$

$$ee_{pos} == 20.8694 + 11.3576 F1 + 0.9598 F2 + 1.2636 F3 + 1.2241 F4$$

Synthetic Output

$$ee = \text{clip}_{0,100}(p \cdot ee_{pos})$$

Where $\text{clip}_{0,100}(x) = \min(100, \max(0, x))$ to conform to the physical range of ee.

Model Evaluation: Due to the limited sample size (n=13), Leave-One-Out Cross-Validation (LOOCV) was used to evaluate generalization capability. The Two-part model achieved an LOOCV RMSE (Expected ee) of 28.415, outperforming the single-stage linear model and demonstrating that the two-part structure robustly handles zero-inflation. Results indicate that F1 and F2 show the maximum positive contribution to the success probability, aligning with the mechanistic expectation that an effective chiral skeleton and complete steric pocket are prerequisites for high ee.

6.3 Two-part (Saturation-aware) Model for Regioselectivity (Ratio 3:4)

The regioselectivity indicator, Ratio(3:4), exhibited a significant **ceiling/saturation** phenomenon (many entries reached the measurement upper limit of >20:1).

2026 SSI You High School Science Award
仅用于2026年成桐中学科学奖论文公示

Traditional linear regression underestimates trends in the high-selectivity region due to this cutoff.

- **Part 1: High Regioselectivity State (Probability of reaching the ceiling)**

  Define high selectivity indicator: $\mathrm{H} = 1(\mathrm{R} \geq 20)$

  Estimate the probability of reaching the upper limit using logistic regression:

  $$\mathrm{p} = \Pr(\mathrm{S} = 1) = \frac{1}{1 + \exp(-\mathrm{z})}$$

  $$\mathrm{z} = \alpha_0 + \alpha_1 \mathrm{F1} + \alpha_2 \mathrm{F2} + \alpha_3 \mathrm{F3} + \alpha_4 \mathrm{F4}$$

- **Part 2: Lower-range ratio regression**

  For values below the saturation limit, a Ridge linear regression estimates the exact ratio.

  $$\mathrm{R}_{low} = \beta_0 + \beta_1 \mathrm{F1} + \beta_2 \mathrm{F2} + \beta_3 \mathrm{F3} + \beta_4 \mathrm{F4}$$

  Synthetic Output

  $$R = \mathrm{clip}_{0,20}(p \cdot 20 + (1 - p) \cdot R_{low})$$

  Where $\mathrm{clip}_{0,20}(x) = \min(20, \max(0, x))$

The two-part saturation model yielded an LOOCV RMSE of 4.3113, proving it can robustly describe the differences between the high-selectivity plateau and the lower-selectivity range.

2026 S.-T. Yau High School Science Award
仅用于2026丘成桐中学科学奖公示

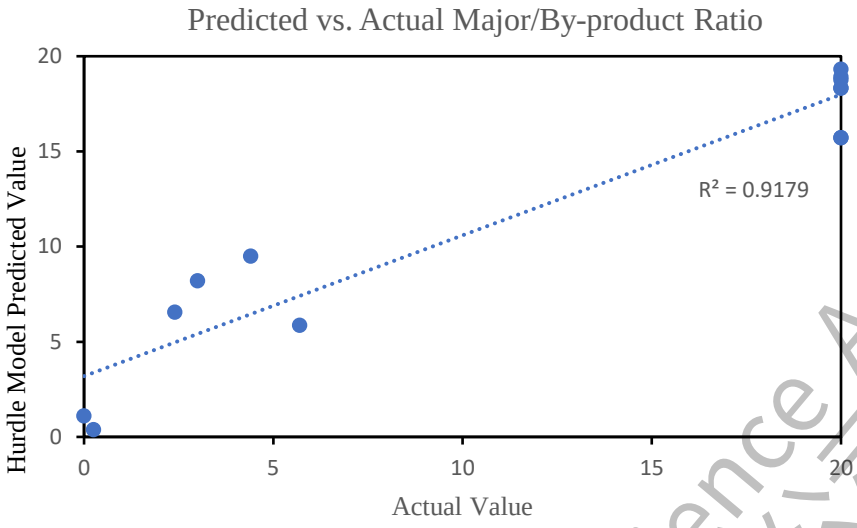


Figure 13. Predicted vs. Actual Ratio of 3:4

6.4 Model Applicability and Extension

This model is highly accurate for predicting product ratios and enantiomeric excess within this Rh(I) catalytic system. If applied to different systems (e.g., varying catalysts or solvents), the correction coefficients in the formula must be refitted, but the overall framework remains robust. With more experimental data, this model can be upgraded to incorporate machine learning algorithms handling variables like ligand concentrations and base types, further broadening its predictive scope.

2026 S.-T. Yau High School Science Award
仅用于2026丘成桐中学科学奖论文公示

7. Conclusion

In the Rh(I)-catalyzed asymmetric cyclization of arylboronates and asymmetric alkynes, optimal catalytic performance requires a hierarchical design approach: **First, select the skeleton → Second, tune the sterics → Third, refine the electronics → Finally, adjust the temperature.**

The rigidly structured bicyclo[2.2.1]heptadiene framework combined with symmetric, moderately bulky, electron-rich aryl substituents constitutes the ideal chiral ligand architecture, achieving simultaneous optimization of regioselectivity (>20:1), enantioselectivity (97.5% ee), and isolated yield (>99%).

References

- Wei-Sian Li; Ting-Shen Kuo; Ping-Yu Wu; Chien-Tien Chen; Hsyueh-Liang Wu. Org. Lett. 2021, 23 (3), 1141–1146.
- Shintani, R.; Okamoto, K; Hayashi, T. Chem. Lett. 2005, 34, 1294.
- Chang-Xue Gu; Wen-Wen Chen; Ming-Hua Xu, J. Org. Chem. 2020, 85, 3887−3893.
- Zhou, F.; Yang, M.; Lu, X. Org. Lett. 2009, 11 (6), 1405-1408.
- Yang, M.; Zhang, X.; Lu, X. Org. Lett. 2007, 9 (24), 5131-5133.

Appendix

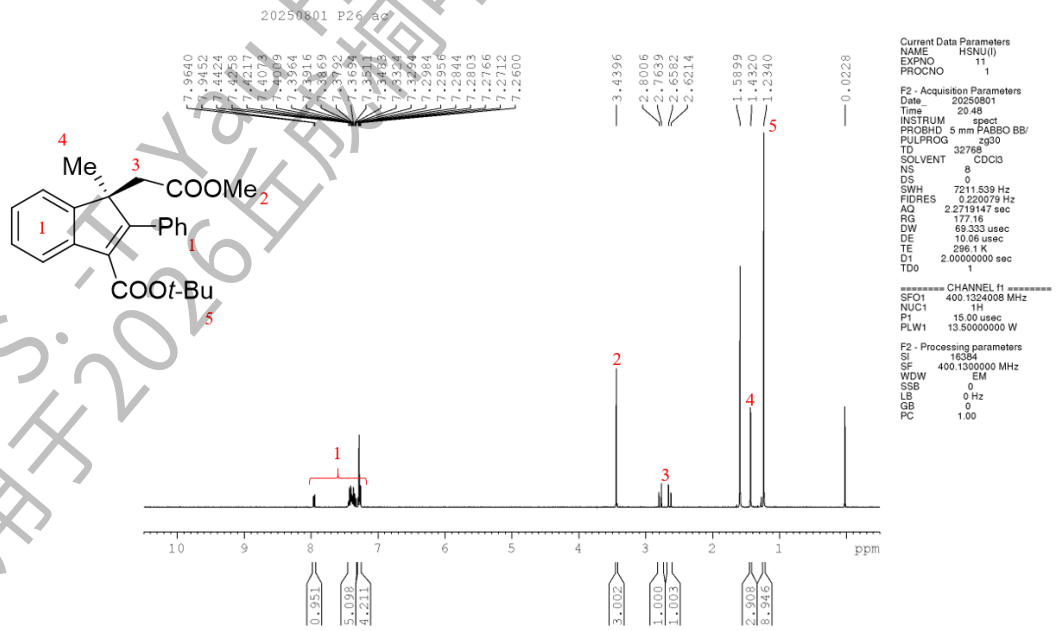


Figure 14. 1H NMR spectrum of product 4

2026 S. T. Yau High School Science Award 仅用于2026丘成桐中学科学奖公示